High-pressure Raman study of the N_2 stretching vibration in argon-nitrogen mixtures at room temperature

T. Westerhoff and R. Feile*
Institut für Physik, Johannes-Gutenberg-Universität, D-55099 Mainz, Germany
(Received 6 March 1996)

We present room-temperature Raman investigations of the nitrogen molecule stretching vibration in $Ar_{1-x}(N_2)_x$ from $x=1$ to $x=0.59$ in the pressure range $1 \leqslant p \leqslant 31$ GPa. Ar substitution leads to an inhomogeneous broadening of the vibrational signal. The β-δ phase transition of pure N_2 is shifted to higher pressures for $x=0.75$. The substituted Ar atoms preferentially occupy the $2a$ sites of the cubic elementary cell of the orientationally disordered δ phase. This interpretation of the experimental data is supported by our model calculations. For $x=0.75$ a superstructure forms in which all the a sites are occupied by Ar atoms. No direct experimental evidence is found for a disorder-order δ-ϵ phase transition observable in pure N_2. However, calculated orientational potential energy barriers propose freezing of the orientational dynamics at reduced pressures. [S0163-1829(96)07626-6]

The mixed system $Ar_{1-x}(N_2)_x$ is well known only for ambient pressures and low temperatures, and many authors have contributed to the understanding of this system (see Ref. 1 and references therein). There, the miscibility of the two compounds over the full concentration range was reported by Barrett and Meyer[2] and later confirmed by Klee and Knorr.[3] The large variety of solid phases of nitrogen (see phase diagram in Ref. 4) plays an essential role for the properties of the mixed system. When reducing the temperature to 63 K without application of pressure nitrogen solidifies into the orientationally disordered hexagonal β phase (space group $P6_3/mmc$) where the axis of the N_2 molecules tumbles around the hexagonal c axis, stabilizing the almost perfect close-packed structure. At 35.6 K the β phase transforms into the orientationally ordered cubic α phase (space group $Pa3$). The phase transition is of first order and of martensitic type. Substitution of the aspherical N_2 dumbbells by spherical Ar atoms strongly affects the transition. The transition temperature is lowered significantly and the transition is smeared out over a large temperature interval.[3] Below a critical nitrogen concentration of $x_c=0.8$ the structural phase transition is totally suppressed, yielding a so-called orientational glass[1] in which the molecular centers of mass still form a hexagonal lattice with the orientations of the N_2 molecules, however, being randomly distributed.

For higher pressures along the 300 K isotherm[4] the p-T phase diagram of pure nitrogen exhibits two structural solid-solid phase transitions. Around 5 GPa the β phase transforms into the cubic δ phase (space group $Pm3n$) which is orientationally disordered as well. The elementary cell contains eight molecules, two on the a and six on the c, respectively. Different types of orientational disorder are reported for the N_2 molecules on the two crystallographic sites. Molecules on the a sites display spherical disorder—e.g., their orientations sample over full spheres—whereas the molecules on the c sites display disklike disorder with their orientations sampling over flat disks.[5,6] N_2 molecules on these sites give rise to two different vibronic frequencies. The higher-frequency component labeled ν_1 is attributed to the a sites and the lower-frequency one labeled ν_2 to the c sites. The latter is 3 times larger in intensity, reflecting the multiplicity of the two sites in the cubic elementary cell. Increasing pressure the cubic δ phase distorts into the lower symmetry orientationally ordered trigonal ϵ phase (space group $R\bar{3}c$) at 16.3 GPa.[7] In our recent Raman study[8,9] of pure nitrogen we observed three contributions to the vibrational band in the ϵ phase as the lower-frequency line ν_2 exhibits a splitting into two components just above the phase transition which increases with increased pressure.

The motivation for the present work is driven by the questions of what happens to the β-δ and the δ-ϵ phase transition of nitrogen in the mixed system, and how these structures are possibly influenced when Ar atoms are added to the nitrogen lattice at higher pressures. The effect of helium admixing on the high pressure phases of nitrogen has already been investigated.[10,11] Vos and Schouten[10] found that fluid helium can be dissolved in ϵ-N_2, favoring this phase, such that the δ-ϵ phase transition occurs at pressures half as high compared to pure N_2 at comparable temperature. The β-δ phase transition was reported not to be shifted at all by the admixture of helium. Raman spectroscopy of the internal stretching vibration of the N_2 molecule served as a sensitive tool for the exploration of the N_2 high-pressure phase diagram[4,5,12–14] besides x-ray experiments[6,7,15] and therefore was used also in this investigations of the mixed system. Preliminary results of our work on this mixed system are published in Ref. 16. Two more samples with different concentration were added so that five different compositions from $x=0.87$ down to $x=0.59$ have been examined (Table I) and compared to our experimental results on pure nitrogen published elsewhere.[9]

Gases of purity better than 99.9997% for Ar and

TABLE I. List of investigated $Ar_{1-x}(N_2)_x$ concentrations and errors.

x	1	0.87	0.86	0.79	0.74	0.59
Δx	–	0.003	0.013	0.04	0.01	0.01

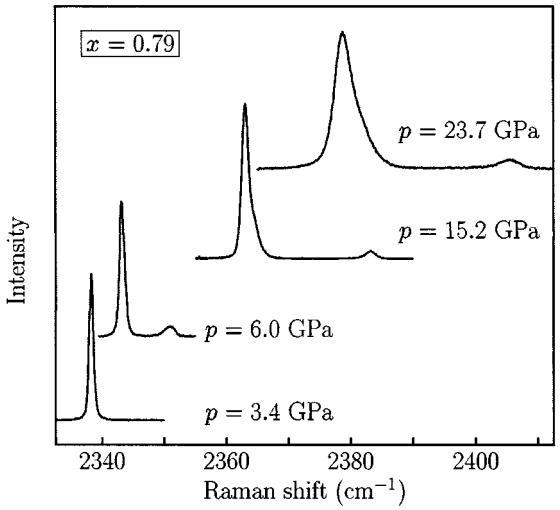

FIG. 1. Spectra of the N_2 vibrons in $Ar_{0.21}(N_2)_{0.79}$.

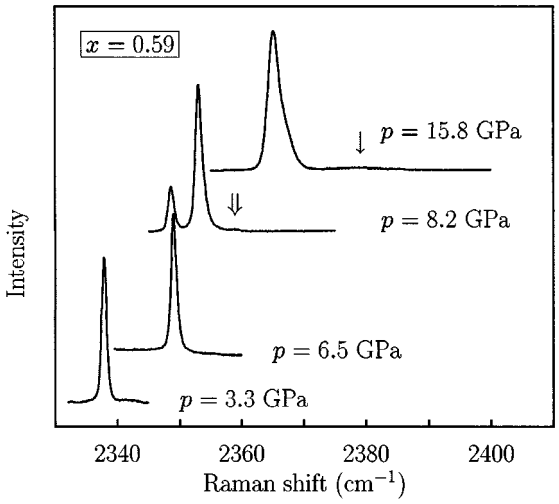

FIG. 2. Spectra of the N_2 vibrons in $Ar_{0.41}(N_2)_{0.59}$; for the arrows see explanation in the text.

99.9995% for N_2 were mixed at room temperature to the appropriate composition and filled into the diamond anvil cell (DAC) designed by Chopelas and Boehler[17] with a high-pressure gas loading system.[18] Pressure was determined *in situ* by the ruby fluorescence method after Mao *et al.*[19] on small ruby chips embedded in the sample. The pressure gradient in the sample was determined from locally separated ruby chips and the well-known pressure dependence of the N_2 stretching vibration probed at different spots across the sample volume at constant pressure. According to these pressure gradients the errors in pressure are estimated to ± 0.1 GPa for $p<8$ GPa, ± 0.8 GPa for $8<p<20$ GPa, and ± 2 GPa for $p>20$ GPa.

The 514.5 nm emission of an Ar ion laser was used as the light source in our experiment. The laser with a typical power of 200 mW was focused to 12 μm diameter onto the samples. The power was reduced to 0.5 mW for the fluorescence measurements on the ruby chips to avoid heating. Backscattered light was analyzed using a Jobin-Yvon U-1000 double monochromator in a standard setup. The actual sampling volume of 3–6 μm in diameter was determined by the collection optics and the 70 μm width of the entrance slit of the monochromator chosen for the frequency resolution in our experiment. This also led to a decrease of the scattering volume along the optical axis, reducing the second-order Raman signal of the diamond anvils in the same frequency range. Prior to each measured spectrum a neon discharge lamp was used to calibrate the frequency and to determine the instrumental resolution function [full width at half maximum (FWHM): 0.6 cm^{-1}].

Five samples of $Ar_{1-x}(N_2)_x$ with different compositions (Table I) have been investigated. Figure 1 representatively shows the Raman signal of the N_2 stretching vibration in the sample with $x=0.79$ at different pressures. At 3.4 GPa an almost symmetric single line is observed. Increasing pressure leads to a splitting of the line around 5 GPa, which becomes larger when pressure is further increased. The asymmetry of the lower-frequency line obvious in the spectrum recorded at a pressure of 15.2 GPa is already observable at pressures around 10 GPa and increases strongly for pressures between 15.2 and 23.7 GPa. The spectra of the $x=0.87$, $x=0.86$, and $x=0.74$ samples display similar pressure dependence. The behavior is quite different in the $x=0.59$ sample (Fig. 2). A single line is still observable at a pressure of $p=6.5$ GPa. The spectrum recorded at a pressure of 8.2 GPa exhibits a splitting which at first glance does not resemble the splitting into ν_1 and ν_2 as seen in pure N_2 or, similarly, in the other mixtures at this pressure. Barely seen, a third vibrational contribution is located at ≈ 2380 cm^{-1} (double arrow in Fig. 2). The frequency difference between this third and the low-frequency line is comparable to that of ν_1 and ν_2 in pure N_2. The intensity of the line in the middle strongly decreases with pressure. At higher pressure (15.8 GPa) a broad line with a strong asymmetry remains whose frequency approximately coincides with that of the ν_2 vibron in N_2 and the other mixed samples. Around 2380 cm^{-1} a broad contribution with low intensity (single arrow in Fig. 2) is noticed.

Spectra of the N_2 vibration in samples within the concentration range $0.74 \leqslant x \leqslant 1$ recorded at comparable pressures around 10 GPa are presented in Fig. 3. Since the vibrational spectra of the mixed samples are in a qualitative agreement with that of pure nitrogen, the two observed lines are labeled as in pure nitrogen with ν_1 for the high- and ν_2 for the low-frequency one. In comparison to N_2 the vibrational spectra in the mixed samples exhibit an asymmetry on the high-frequency side of ν_2 and a smaller one on the low-frequency side of ν_1. The decrease in intensity for the ν_1 vibron with increasing Ar admixture is obvious. In the $x=0.74$ sample the ν_1 vibron intensity has almost vanished.

At small pressure the widths of the vibrational lines were found to be in the same order of magnitude as the width of the resolution function. For a detailed line shape analysis we convoluted the theoretical line shape function with the experimentally determined resolution function and fitted this new function to the experimental data with a standard Marquardt χ^2 algorithm.[20] At higher pressures, where the vibrons in the mixed system are significantly broader than the resolution function, this convolution method was still used for the fitting to ensure comparability of the obtained linewidths data. Two line shape functions, a single Gaussian

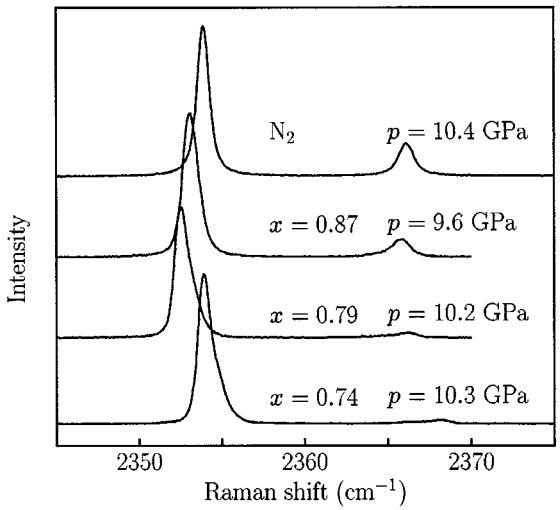

FIG. 3. Spectra of the N_2 vibrons of four different concentrations in $Ar_{1-x}(N_2)_x$ at a pressure of ≈ 10 GPa.

and a single Lorentzian and their superpositions have been tested, carefully checking the deviations between the fit function and the experimental data.[8] For pressures below 5 GPa Lorentzians gave the best results. At higher pressures the broad and asymmetric line shape of the vibrons obviously demands the fitting with a superposition of two line shape functions. Here, the superposition of two Gaussians had to be favored when comparing the deviations from the experimental data. This superimposed line shape function was used for the fitting of the N_2 vibrons in all mixtures investigated for pressures above 5 GPa. The fitting parameters obtained for the frequencies were corrected with respect to the frequency of a well-known line of a neon discharge lamp, also used to determine the experimental resolution function. Figure 4 presents the pressure dependence of the N_2 vibrational frequencies in the $x = 0.79$ sample. The solid lines included in Fig. 4 are fits to the pressure dependence of the vibrons in pure nitrogen as presented in Ref. 9 for comparison. The overall agreement of the vibrational frequencies in the mixed samples with the N_2 data is obvious. The β-δ phase transition is observed by the splitting of the vibron around 5 GPa as in pure nitrogen. In contrast to pure nitrogen the observed asymmetric line shape demanded fitting of both vibrons with a superposition of two lines for all pressures investigated. The individual components are labeled as given in Fig. 4. Different pressure scans gave comparable results and are therefore not indicated separately. The vibrational frequencies in the $x = 0.59$ sample are given in Fig. 5, together with the results in pure N_2. The missing splitting of the vibron at 6.5 GPa shown in Fig. 2 is consequently reflected in the fitting results for the frequencies (Fig. 5). The frequencies of the two lines fitted to the vibron observed between 3.4 and 6.5 GPa (ν_a and ν_b) match the frequency of the vibron in β-N_2 at lower pressures. For $p > 5$ GPa the vibron frequencies of the β phase can be extrapolated from below. The low-frequency line in the spectra between 8.2 GPa and 12.8 GPa and the large intensity line in the spectrum at 15.8 GPa coincide with the frequency of the ν_2 vibron in pure N_2. The tiny contribution labeled with a double arrow in Fig. 2 was fitted with a single Gaussian function and its frequency

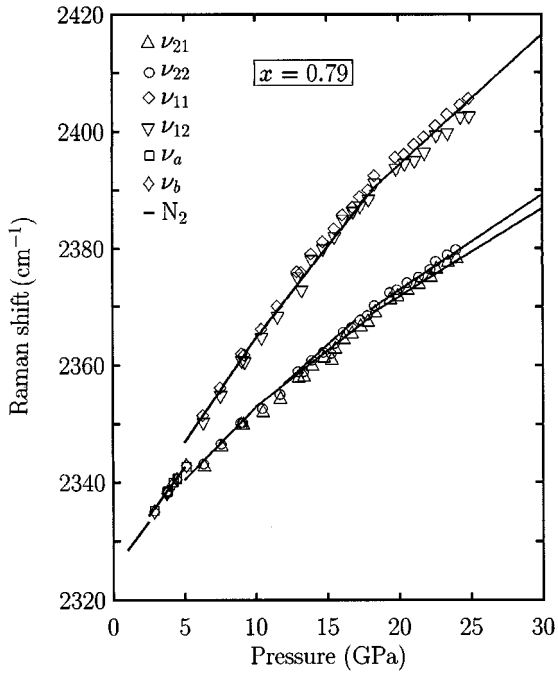

FIG. 4. Frequencies of the N_2 vibrons in $Ar_{0.21}(N_2)_{0.79}$ vs pressure. The solid lines are fits to the N_2 data presented in Ref. 9. Errors in frequencies are smaller than the size of the symbols; for the errors in pressure see text.

matches that of the ν_1 vibron in pure N_2. The broad structure denoted by a single arrow in Fig. 2 was fitted with a superposition of two Gaussian functions. The component higher in frequency also coincides with the ν_1 vibron in

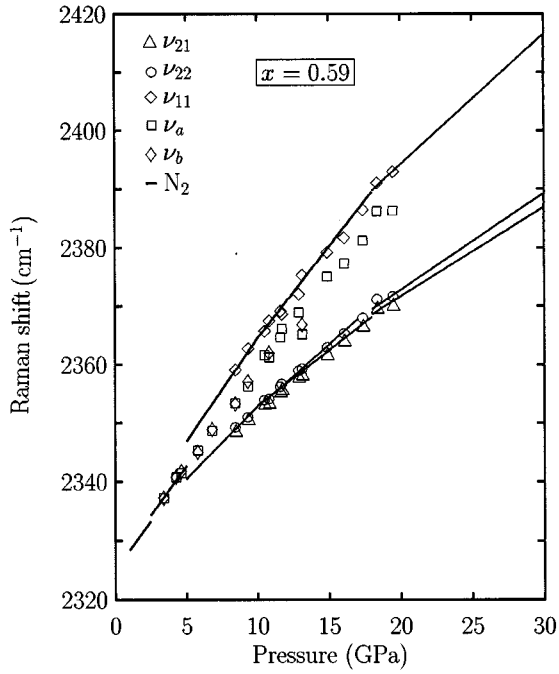

FIG. 5. Frequencies of the N_2 vibrons in $Ar_{0.41}(N_2)_{0.59}$ vs pressure. The solid lines are fits to the N_2 data presented in Ref. 9. Errors in frequencies are smaller than the size of the symbols; for the errors in pressure see text.

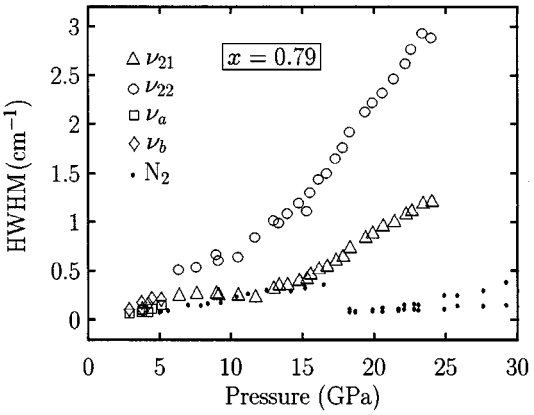

FIG. 6. Half widht at half maximum (HWHM) (Γ) of ν_{21}, ν_{22}, ν_a, and ν_b in $Ar_{0.21}(N_2)_{0.79}$. Errors in Γ are smaller than the size of the symbols; for the errors in pressure see text.

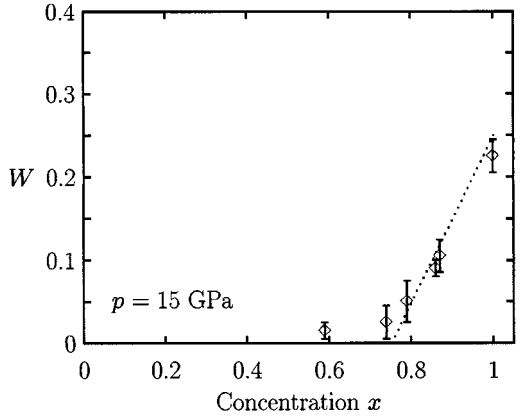

FIG. 8. Weighted intensity ratio $W = xI(\nu_1)/[I(\nu_1)+I(\nu_2)]$ at 15 GPa vs concentration. For the dotted line see discussion in the text.

N_2, whereas the frequency of the other component again follows the pressure dependence of the vibron frequency of β-N_2 extrapolated to higher pressures.

The pressure dependence of the linewidths for ν_a, ν_b, ν_{21}, and ν_{22} is shown in Fig. 6. Here, the β-δ transition at 5 GPa is marked by a small step in the linewidths. In the δ phase above 10 GPa the widths of ν_{21} and ν_{22} increase monotonously with pressure, much more pronounced for the latter. For comparison the data for ν_{21} and ν_{22} of pure N_2 published in Ref. 9 are included in Fig. 6. The drop of those data between 16.5 and 18 GPa marks the $\delta-\epsilon$ phase transition in pure N_2. The linewidths of both components in the mixed system with $x=0.79$ are larger than those in pure nitrogen. Figure 7 compares the linewidths data in all investigated samples at a pressure of 15 GPa. The widths increase with the Ar concentration, and $\Gamma_{\nu_{22}}$ is always about twice as broad as $\Gamma_{\nu_{21}}$ in the mixed samples.

For a quantitative analysis of the decrease in intensity of the ν_1 vibron with increasing Ar admixture (see Fig. 3), we calculated the weighted intensity ratio

$$W = x\frac{I(\nu_1)}{I(\nu_1)+I(\nu_2)},$$

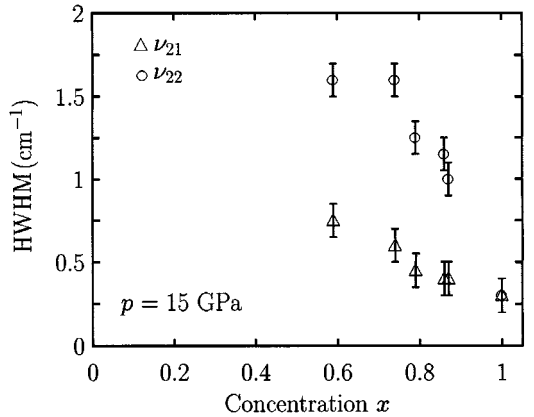

FIG. 7. HWHM of the N_2 vibrons ν_{21} and ν_{22} at a pressure of 15 GPa vs concentration. For errors in concentration see Table I.

where x denotes the N_2 concentration, and $I(\nu_1)$ and $I(\nu_2)$ the integrated intensities of the two vibrons. This ratio measures the contribution of the intensity of the ν_1 vibron to the total intensity scattered into the vibron band. Thus, it is proportional to the number of a positions in the sample occupied by N_2 molecules relative to the total number of positions in the sample at a given concentration. In pure nitrogen the ratio $W=0.25$ reflects the multiplicities of the two sites in the elementary cell ($2a$ and $6c$). Replacing the N_2 molecules on the two sites a and c statistically with Ar atoms, this value would be maintained, whereas a preferred substitution of one site would result in a deviation from this value. Obviously, the experimental data presented in Fig. 8 display an almost linear decrease with increasing Ar concentration. The data perfectly match within the limits of their errors with the dotted line which represents the case that the Ar atoms favor the a positions on which (in pure N_2) the N_2 molecules exhibit spherical disorder. For $x=0.75$ ideally all a positions are occupied by Ar and the mixed system $Ar_{0.25}(N_2)_{0.75}$ forms a superstructure.[16]

The geometrically plausible preference of the spherical Ar atoms for the a positions in the δ phase in the mixed system is also supported by the results of model calculations.[8] In Ref. 21 we reported on calculations of single-particle orientational potentials for the N_2 molecules at the two different crystallographic sites in the cubic lattice of δ-N_2. For a reference molecule its interaction energy with its neighboring molecules (of which the orientations were averaged over spheres or disks of appropriate orientation) was calculated as a function of its own orientation. The single-molecule orientational potential obtained in this way showed characteristic differences for the two sites. With the pressure dependence of the orientational potential barriers we were able to construct phase boundary lines in the p-T phase diagram of nitrogen.[21]

Now we apply these calculations to determine the gain in energy, when replacing N_2 molecules by Ar atoms on the a or c sites in the cubic lattice of δ nitrogen. To calculate the interaction energy between nitrogen and Ar a simple Lennard-Jones 6-12 atom-atom potential was used, replacing the interaction potential for the N_2 molecules given by Etters *et al.*[22] used otherwise. The Lennard-Jones parameters are

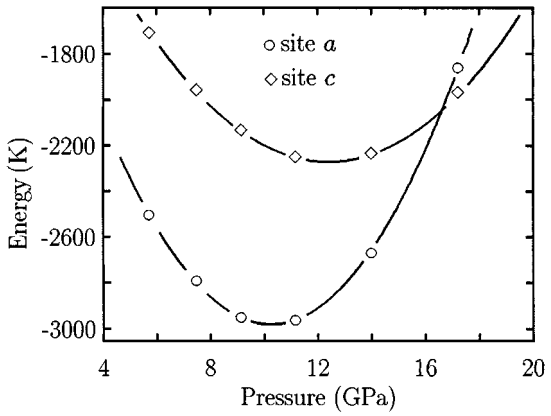

FIG. 9. Energy difference between occupation of the two sites a or c with Ar atoms or N_2 molecules, respectively as a function of pressure. Solid lines are guides to the eye.

taken from Ref. 23 with $\epsilon_{\text{Ar-N}}=67.15$ K and $\sigma_{\text{Ar-N}}=3.35$ Å. In a first run the orientational potential was calculated for Ar as a reference atom at several pressures within the stability regime of the δ phase, yielding single energy values for each pressure (the spherical Ar atom cannot show any angular dependence). The calculations were repeated for the same pressures with an N_2 molecule as a reference molecule and with the nitrogen-nitrogen interaction potential of Ref. 22. The resulting orientational potential exhibits a modulation in the energy depending on the orientation of the reference molecule above a positive offset in energy which is large compared to this modulation. The large positive energy values for this offset in the orientationl potential are due to the fact that the δ phase is only stable at high pressures. For the resulting small distances in the lattice the interaction potential becomes strongly repulsive. We calculated a thermal average of the orientation potential modulation with a temperature of 300 K used in the Boltzmann factor. This average value was added to the offset to give the average potential of an N_2 molecule on position a. The differences between this value and the energy value determined for the Ar atom sited at the reference position are shown in Fig. 9. The gain in energy (negative energy values) is always larger for substituting the N_2 molecules on the a sites than on the c sites for pressures within the stability range of the cubic δ phase, in agreement with the experimental findings.

As mentioned above, we previously were able to investigate the pressure dependence of the orientational potential barriers for the N_2 molecules in the δ phase of pure nitrogen. In the following we apply these calculations to investigate the pressure dependence of the potential barriers for N_2 molecules at position c in two Ar-doped N_2 lattices of different compositions. For these calculations we assumed that the Ar atoms prefer the a positions in the lattice of δ-N_2 according to theresults presented above. Substituting N_2 molecules on all the a positions by Ar atoms yields a sample with the concentration of $x=0.75$ due to the multiplicity of the two sites in the cubic elementary cell. For the second Ar-doped lattice we replaced only one N_2 molecule by an Ar atom in the second-neighbor shell of the reference molecule sitting at position c. This second-neighbor shell is built up by four a positions (the first-neighbor shell contains two c positions).

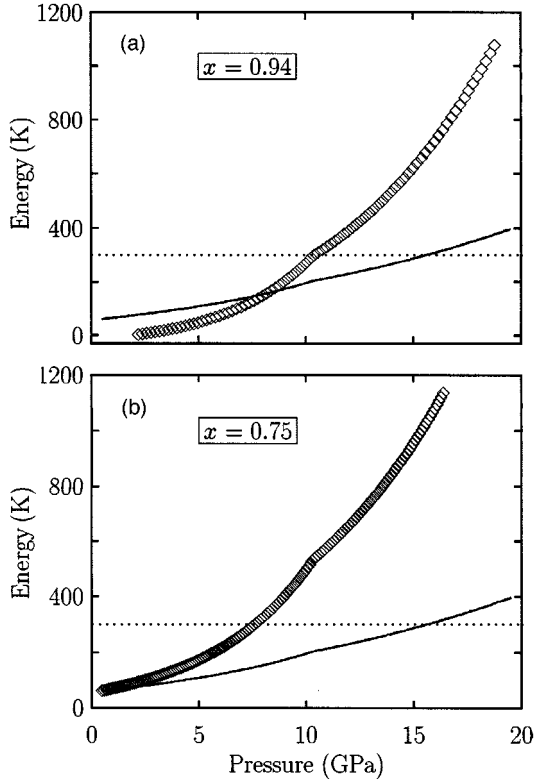

FIG. 10. Barriers of the orientational potential at position c in $Ar_{1-x}(N_2)_x$ for $x=0.94$ (a) and $x=0.75$ (b) vs pressure. The solid lines give the barriers in pure nitrogen for comparison (see Ref. 21).

This doping procedure yields a configuration which is the most probable for a sample with the concentration of $x=0.94$. The orientational potential of these two lattices have been calculated together with the pressure dependence of the barriers important for the orientational dynamic of the N_2 molecule. The results are presented in Fig. 10. The solid line includes the pressure dependence of the orientational potential barriers obtained in a pure nitrogen lattice.[21] Obviously, the barriers in the Ar-doped lattice increase much stronger with the pressure than the barriers in pure nitrogen. For the interpretation we follow the discussion in Ref. 21. There we argued that, since the rotational constant of the nitrogen molecule $B_0=2.89$ K (Ref. 24) is much smaller than any temperature within the stability region of the δ phase, the rotator can be treated classically. Therefore, in a system with a thermal energy of 300 K a barrier with a height of 300 K is interpreted as a limit for the freezing of the orientational dynamics. At room temperature in pure nitrogen the barrier exceeds the limit at a pressure around 17 GPa in coincidence with the pressure of the δ-ϵ phase transition along the 300 K isotherm. In the Ar-doped lattice we find a reduction of the freezing pressure to 10 GPa for $x=0.94$ and a further, but smaller, one to ≈ 7.5 GPa for $x=0.75$.

We now want to discuss the consequences of the experimental and theoretical results for the two phase transitions of nitrogen under investigation in the mixed system. These results are summarized in Fig. 11. The β-δ and δ-ϵ phase transitions in pure N_2 ($x=1$) as known from the literature are denoted by (○) and (◇), respectively. The highest pres-

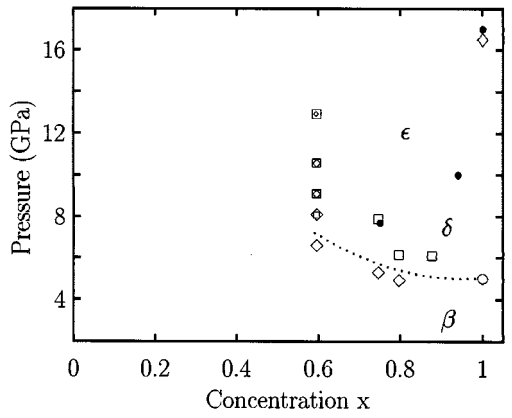

FIG. 11. Room-temperature high-pressure phase diagram of $Ar_{1-x}(N_2)_x$. The experimentally determined β-δ and δ-ϵ transitions pressures in pure N_2 ($x=1$) are denoted by (○) and (◇), respectively. (◇) indicate the upper pressures boundaries of pure β and (□) the lower boundaries of pure δ vibrational spectra. The size of the symbols at $x=0.59$ scales with the relative intensities of β and δ vibrons in the transformation regime. The dotted line guides the eye for the β-δ phase boundary. Freezing pressures obtained from the orientational potential calculation in the δ phase are marked by (●).

sures where we could observe vibrational spectra of the β phase and the lowest pressures for those spectra of the δ phase are denoted by (□) and (◇). At $x=0.59$ the spectra of both phases were observed over a large pressure regime with their relative intensity indicated by the different size of the two symbols. The β-δ phase transition is clearly shifted to a higher pressure for this concentration, but more or less independent on the concentration for $x>0.75$. In the pressure range of the cubic δ phase, the Ar atoms, in the mixed system, prefer the *a* positions for concentrations with $x\geqslant 0.75$. Below that concentration the Ar atoms have to occupy *c* positions also. At the concentration of $x=0.59$ each elementary cell of δ-N_2 statistically contains at least one Ar atom located on position *c*. Obviously, the mixed system with a 16% ''overload'' of spherical particles favors the more or less closed packed hexagonal β structure over the cubic δ structure stable for pure N_2 at comparable pressures. Further measurements on samples with smaller nitrogen concentrations are necessary to answer the question whether the β-δ transition may be totally suppressed as found in this system at ambient pressure and low temperature.

The characteristic feature of the N_2 δ-ϵ phase transition, the drop of the vibrational linewidths by ≈ 0.5 cm^{-1} [see (●) in Fig. 6], was not observed for any of the mixed samples investigated. On the contrary, the linewidths increase monotonously with pressure for all those samples. A drop in the widths of similar size must have been detectable in the mixtures, since the values of the linewidths are found to be between 0.4 and 1.6 cm^{-1} (depending on the concentration) at the pressure of 15 GPa (see Fig. 7). The disorder-order δ-ϵ transition in pure N_2 is accompanied by a complete freezing of the molecular orientational degrees of freedom around 17 GPa. At this pressure the barriers of the calculated orientational potentials are to large to be crossed by the molecules. Introducing Ar, the local environments of the N_2 molecules are changed drastically. The potential barriers are increased and the freezing of the molecular orientations is expected already at lower pressures $p\approx 10$ GPa for $x=0.94$ and $p\approx 7.5$ GPa for $x=0.75$ at a temperature of 300 K. The so-determined freezing pressures of the orientational dynamics are included in Fig. 11 with (●) yielding rather a small stability regime for the δ phase in the p-x plane at room temperature. Since we cannot distinguish the δ and the ϵ phase by means of our experimental data, the existence of the ϵ phase remains questionable for the mixed samples. Experiments with small doping should clarify this strong influence of Ar substitution.

In summary, with Raman data on the N_2 stretching vibration and model calculations of orientational potentials for the N_2 molecules in the δ phase we were able to construct a x-p phase diagram of $Ar_{1-x}(N_2)_x$ at room temperature. The β-δ phase transition is shifted to higher pressures for $x\leqslant 0.75$. The Ar atoms preferentially occupy the positions with spherical disorder of the N_2 orientations in the δ phase. The freezing of the orientational dynamic associated with the δ-ϵ transition may occur already at smaller pressures in the mixed system.

This work was supported by the ''Deutsche Forschungsgemeinschaft'' (SFB 262) and the ''Materialwissenschaftliches Forschungszentrum der Universität Mainz.'' We thank A. Zerr and R. Boehler for their support in diamond-anvil-cell high-pressure measurements. We thank K. Binder, F. Bruchhäuser, M. Müser, P. Nielaba, and E. Sherman for valuable discussions.

*Present and corresponding address: Institut für Festkörperphysik, Technische Hochschule Darmstadt, Hochschulstraße 8, D-64289 Darmstadt, Germany.

[1] U. T. Höchli, K. Knorr, and A. Loidl, Adv. Phys. **39**, 405 (1990).
[2] C. S. Barrett and L. Meyer, J. Chem. Phys. **1**, 107 (1965).
[3] H. Klee and K. Knorr, Phys. Rev. B **42**, 3152 (1990).
[4] H. Schneider, W. Häfner, A. Wokaun, and H. Olijnyk, J. Chem. Phys. **96**, 8046 (1992).
[5] R. LeSar *et al.*, Solid State Commun. **32**, 131 (1979).
[6] D. T. Cromer, R. L. Mills, D. Schiferl, and L. A. Schwalbe, Acta Crystallogr. B **37**, 8 (1981).
[7] H. Olijnyk, J. Chem. Phys **93**, 8968 (1992).
[8] T. Westerhoff, Ph.D. thesis, Institut für Physik, Universität Mainz, 1995.
[9] T. Westerhoff, A. Wittig, and R. Feile, Phys. Rev. B **54**, 14 (1996).
[10] W. L. Vos and J. A. Schouten, Phys. Rev. Lett. **64**, 898 (1990).
[11] J. A. Schouten, Phys. Rep. **172**, 33 (1989).
[12] S. Buchsbaum, R. L. Mills, and D. Schiferl, J. Phys. Chem. **88**, 2522 (1984).
[13] D. Schiferl, S. Buchsbaum, and R. Mills, J. Phys. Chem. **89**, 2324 (1985).
[14] R. Reichlin *et al.*, Phys. Rev. Lett. **55**, 1464 (1985).
[15] R. L. Mills, B. Olinger, and D. T. Cromer, J. Chem. Phys. **84**, 2837 (1986).
[16] T. Westerhoff, F. Bruchhäuser, R. Feile, and R. Boehler, J. Non-Cryst. Solids **172-174**, 481 (1994).
[17] A. Chopelas and R. Boehler, Mater. Rev. Soc. Sym. Proc. **22**, 275

(1984).
[18] R. L. Mills, D. H. Liebenberg, J. C. Bronson, and L. C. Schmidt, Rev. Sci. Instrum. **51**, 891 (1980).
[19] H. K. Mao, P. M. Bell, J. W. Shaner, and D. J. Steinberg, J. Appl. Phys **49**, 3276 (1978).
[20] P. R. Bevington, *Data Reduction and Error Analysis for the Physical Sciences* (McGraw-Hill, New York, 1969).
[21] T. Westerhoff and R. Feile, Z Phys. B **100**, 417 (1996).
[22] R. D. Etters, V. Chandrasekharan, E. Uzan, and K. Kobashi, Phys. Rev. B **33**, 8615 (1986).
[23] M. H. Müser, W. Helbing, P. Nielaba, and K. Binder, Phys. Rev. E **49**, 3956 (1994).
[24] G. Herzberg, *Spectra of Diatomic Molecules* (van Nostrand Reinhold Company, New York, 1950).